

Distributed Communication-Aware Coverage Control by Mobile Sensor Networks [★]

Yiannis Kantaros ^a, Michael M. Zavlanos ^a

^a*Department of Mechanical Engineering and Materials Science, Duke University, Durham, North Carolina-27708, U.S.A.*

Abstract

The purpose of this paper is to propose a distributed control scheme to maximize area coverage by a mobile robot network while ensuring reliable communication between the members of the team. The information that is generated at the sensors depends on the sensing capabilities of the sensors as well as on the frequency at which events occur in their vicinity, captured by appropriate probability density functions. This information is then routed to a fixed set of access points via a multi-hop network whose links model the probability that information packets are correctly decoded at their intended destinations. The proposed distributed control scheme simultaneously optimizes coverage and routing of information by sequentially alternating between optimization of the two objectives. Specifically, optimization of the communication variables is performed periodically in the dual domain. Then, between communication rounds, the robots move to optimize coverage. Motion control is due to the solution of a distributed sequential concave program that handles efficiently the introduced nonlinearities in the mobility space. Our method is illustrated in computer simulations.

Key words: Mobile robot networks; communication networks; coverage control; distributed optimization

1 Introduction

The area coverage problem is related to the development of a control plan that allows a group of mobile agents equipped with sensing and communication capabilities to spatially configure themselves in a way that maximizes the cumulative probability that events are detected in an area of interest. While the area coverage problem has recently received a lot of attention, ensuring that the collected rates of information can be efficiently relayed to a desired set of access points for subsequent processing is, to the best of our knowledge, still an open problem. In this paper, we provide a distributed solution to this problem of joint coverage and communication control.

The literature related to coverage problems is quite extensive. In [3], the authors propose a distributed controller based on Lloyd's algorithm for sensing a convex

area. In this work, it is assumed that the sensing performance degrades as the distance from the sensor increases. The case where the robots are equipped with range-limited sensors is discussed in [4]. Distributed controllers for coverage optimization have been proposed in [5] that minimize the energy needed for sensing and data processing. Coverage optimization for anisotropic sensors, whose performance depends on both the distance from the sensor and its orientation, is studied in [6–9], while [10–13] discuss coverage of non-convex areas.

The area coverage problems discussed above typically ignore the requirement that the information collected by the robot sensors needs to be routed to a desired set of destinations. Introducing this capability in the system gives a new twist to the problem on the interface with communication control and networking. Most of the existing approaches to communication control of mobile robot networks employ proximity graphs to model information exchange between robots and, therefore, consider the problem of preserving graph connectivity. Such approaches involve, for example, maximization of the algebraic connectivity of the graph [14, 15], potential fields that model loss of connectivity as an obstacle in the free space [16], tools from reachability analysis to ensure connectivity in networks of mobile sensors [17], and distributed hybrid approaches that decompose con-

[★] This paper was not presented at any IFAC meeting. The material in this paper was partially presented in [1] and [2]. Corresponding author Yiannis Kantaros, yiannis.kantaros@duke.edu

Email addresses: yiannis.kantaros@duke.edu (Yiannis Kantaros), michael.zavlanos@duke.edu (Michael M. Zavlanos).

trol of the discrete graph from continuous motion of the robots [18]. Distributed algorithms for graph connectivity maintenance have also been implemented in [19, 20]. A comprehensive survey of this literature can be found in [21].

A more realistic communication model between mobile robots, compared to the above graph-theoretic approaches, is presented in [22, 23] that takes into account the routing of packets as well as desired bounds on the transmitted rates. In this model, edges in the communication graph are associated with the probability that packets delivered through the corresponding links are correctly decoded by their intended receivers. This formulation gives rise to optimization problems to determine the desired rates and routes. Related methods for the control of wireless robot networks are proposed in [24] and [25], where the wireless channels are modeled using path loss, shadowing, and multi-path fading, or evaluated using on-line techniques, respectively. Similarly, the Signal to Interference ratio (SIR) is utilized in [26] to model communication links between mobile aerial vehicles and ground sensors that perform collaborative tasks.

In this paper, we assume a team of mobile robot sensors responsible for covering a convex area of interest with the additional requirement that the sensory information collected by the robots can be efficiently routed to a desired set of fixed access points (APs). The rate of information generated at every sensor depends on the quality of sensing as a function of the sensing range as well as on the probability that events occur in the vicinity of that sensor, captured by an appropriate probability density function over the area of interest. This information is then routed to the APs via a multi-hop network whose links model the probability that information packets are correctly decoded at their intended destinations.

The key idea in this work is to formulate the area coverage problem as a *constrained optimization problem* in the robot positions, associated area partitions, and routing decisions. We can then use the routing decisions to control the feasible set so that it contains the Voronoi partition as a solution, which is well-known to be optimal for the unconstrained problem [4]. Substituting the Voronoi partition in the constrained problem, we obtain an optimization problem in the robot positions and routing decisions, which we solve in a way similar to our prior work [22]; we decouple coverage and routing control and alternate between optimization of the two objectives. In particular, given a spacial configuration of the robots in the area of interest, the communication variables are updated using a distributed subgradient algorithm in the dual domain. The update of the communication variables is then followed by robot motion in a direction that optimizes the coverage objective. Robot motion is formulated as a distributed sequential concave program, that allows us to handle nonlinearities in the coverage objec-

tive as well as the nonlinear dependence of the communication constraints on the robot positions. As the robots move, the optimal solution in the communication space drifts, which introduces a possible infeasibility gap in the primal variables. While such infeasibility gaps persist, the affected robots remain stationary until feasible routing variables are determined by the optimization in the communication space. Following the analysis in [22], we obtain bounds on the robot velocities that characterize the performance of communications. The proposed control scheme is distributed, utilizing only information that is locally available at the sensors.

The problem of simultaneous coverage and communication control is also addressed in [2], although in a centralized setting. In that work, the routing variables are updated periodically in discrete time while the robot motion is performed along the negative gradient of a function that combines the coverage objective and a barrier potential function to ensure satisfaction of the imposed communication constraints. A related problem that considers the minimization of the aggregate information delivered directly, in one hop, from the robots to a sink node is addressed in [27]. Multi-hop communication in the context of coverage is considered in [28–30]. Specifically, in [28] the objective is to minimize the energy consumption in the network, so paths are sought that ensure this minimum energy objective. In [29, 30] a joint coverage and graph connectivity framework is developed for robots that have limited, proximity-based communication ranges. These latter approaches differ from the one proposed here in that we consider more realistic models of wireless communication that involve routing of information over a network of varying link reliabilities, and we also ensure desired information rates that depend on the frequency with which events occur in the sensors’ vicinity.

The rest of this paper is organized as follows. Section 2 presents the coverage problem in the presence of communication constraints. The proposed control scheme is presented in section 4 while its efficiency is examined in section 6 through a simulation study. Conclusive remarks are provided in the last section.

2 Problem Formulation

Assume a team of N mobile robots responsible for the sensing coverage of a convex and compact area $\mathcal{A} \subset \mathbb{R}^2$ and for the transmission of packets of information to a fixed set of K access points (APs). The positions of all nodes are stacked in the vector $\mathbf{x} = [\mathbf{x}_1^T, \dots, \mathbf{x}_i^T, \dots, \mathbf{x}_{N+K}^T]^T$, where $i \in \{1, \dots, N\}$ for the robots and $i \in \{N+1, \dots, N+K\}$ for the APs. The motion of the robots is assumed to be governed by the first order differential equation:

$$\dot{\mathbf{x}}_i = \mathbf{u}_i, \quad i = 1, \dots, N, \quad (1)$$

where $\mathbf{u}_i \in \mathbb{R}^2$ stands for the control input associated with the i -th robot.

To achieve area coverage, each robot is equipped with an isotropic sensor whose accuracy is captured by a radially decreasing function f that is maximal at the sensor location \mathbf{x}_i . In this context, a larger value of f means better sensing accuracy. In particular, we choose

$$f(\mathbf{x}_i, \mathbf{q}) = e^{-\|\mathbf{q} - \mathbf{x}_i\|^2}. \quad (2)$$

Moreover, let $\phi(\mathbf{q}) : \mathcal{A} \rightarrow \mathbb{R}_+$ be an integrable density function representing the probability that an event takes place at the point $\mathbf{q} \in \mathcal{A}$. Then, the coverage problem can be formulated as follows:

$$\underset{\mathbf{x}}{\text{maximize}} \left[\mathcal{H}(\mathbf{x}) = \int_{\mathcal{A}} \max_{i=1, \dots, N} f(\mathbf{x}_i, \mathbf{q}) \phi(\mathbf{q}) d\mathbf{q} \right]. \quad (3)$$

A common geometric approach to simplify the area cost function \mathcal{H} is via the tessellation of the area of interest into subregions \mathcal{W}_i , $i \in \{1, \dots, N\}$ according to some distance metric, and the assignment of those regions to the robots for sensing purposes. Requiring that $\bigcup_{i=1}^N \mathcal{W}_i = \mathcal{A}$ and that the sets \mathcal{W}_i are disjoint except for their boundary, this approach allows us to reformulate the coverage problem (3) as:

$$\underset{\mathbf{x}, \mathcal{W}}{\text{maximize}} \left[\mathcal{H}(\mathbf{x}, \mathcal{W}) = \sum_{i=1}^N \int_{\mathcal{W}_i} f(\mathbf{x}_i, \mathbf{q}) \phi(\mathbf{q}) d\mathbf{q} \right], \quad (4)$$

where $\mathcal{W} = \{\mathcal{W}_i\}_{i=1}^N$ denotes the collection of regions \mathcal{W}_i assigned to the robots positioned at \mathbf{x} .

The problem that we address in this paper is the optimization of the objective \mathcal{H} in (4), subject to communication constraints required to ensure desired information flows from the sensor robots to the Access Points (APs). In particular, let $r_i \in [0, 1]$ denote the normalized average rate (information units per unit of time) at which the i -th robot generates information. We assume that this rate depends on both the sensing performance over the ϕ -weighted area \mathcal{W}_i and the probability that an event will occur at each point $\mathbf{q} \in \mathcal{W}_i$. Using R_0 to denote the transmission rate of the terminals' radios, the effective rate at which information is generated at sensor i is:

$$r_i(\mathbf{x}_i, \mathcal{W}_i) = R_0 \int_{\mathcal{W}_i} f(\mathbf{x}_i, \mathbf{q}) \phi(\mathbf{q}) d\mathbf{q}. \quad (5)$$

This information is then routed to the APs via a multi-hop network whose links model the probability that information packets are correctly decoded at their intended destinations. Letting $R(\mathbf{x}_i, \mathbf{x}_j)$ denote this probability, that a packet transmitted by the i -th robot is correctly decoded by the j -th node, the effective transmission rate from i to j is $R_0 R(\mathbf{x}_i, \mathbf{x}_j)$. This rate denotes

the rate of information that is successfully conveyed through this link. To simplify notation, we assume all robots use the same transmission rate R_0 . In fact, we hereafter work with normalized rates by making $R_0 = 1$. This means that rates are measured as (dimensionless) fractions of the transmission rate R_0 .

Packets generated at terminal i can be conveyed to the APs either directly, if $R(\mathbf{x}_i, \mathbf{x}_j) > 0$ for $j \in \{N+1, \dots, N+K\}$, or through a multi-hop communication path. We model this process using routing decisions $T_{ij} \in [0, 1]$ that represent the fraction of time that node i communicates with robot j . Upon generation or arrival from another robot, packets are stored in a queue at every robot i and they leave this queue provided they are transmitted and correctly decoded by any other node j . The normalized rate at which packets leave the queue at the i -th node and are sent to node j is $T_{ij} R(\mathbf{x}_i, \mathbf{x}_j)$, where we assume that the transmission and the decoding processes are independent events. Then, the average rate at which packets leave the i -th queue is:

$$r_i^{\text{out}} = \sum_{j=1}^{N+K} T_{ij} R(\mathbf{x}_i, \mathbf{x}_j). \quad (6)$$

Similarly, the average rate at which packets arrive at the i -th queue is:

$$r_i^{\text{in}} = r_i(\mathbf{x}_i, \mathcal{W}_i) + \sum_{j=1}^N T_{ji} R(\mathbf{x}_j, \mathbf{x}_i). \quad (7)$$

Note that the APs can only receive information which explains the upper limits in the sums of equations (6) and (7). To ensure that packets are eventually delivered to the APs, we require that there are no unstable queues in the network. A queuing network is considered unstable if the number of packets stored in the queues grows linearly as $t \rightarrow \infty$, as defined in [31]. Since unstable queuing networks are typically composed of supercritical queues, i.e., queues for which it holds that $r_i^{\text{out}} - r_i^{\text{in}} < 0$, we require that

$$\begin{aligned} c_i(\mathbf{x}_i, \mathcal{W}_i, \mathbf{t}) &= r_i^{\text{out}} - r_i^{\text{in}} \\ &= \sum_{j=1}^{N+K} T_{ij} R(\mathbf{x}_i, \mathbf{x}_j) - \sum_{j=1}^N T_{ji} R(\mathbf{x}_j, \mathbf{x}_i) - r_i(\mathbf{x}_i, \mathcal{W}_i) \geq 0 \end{aligned} \quad (8)$$

for all $i \in \{1, \dots, N\}$ and for all time t , where $\mathbf{t} \in \mathbb{R}^{N(N+K)}$ is a vector that stacks the routing decisions T_{ij} of all robots at time t . Our goal is to determine robot positions \mathbf{x} , an associated partition of the space \mathcal{W} , and routing decisions \mathbf{t} , that optimize the coverage objective \mathcal{H} while ensuring satisfaction of the constraints (8). Note that for a given spatial configuration \mathbf{x} , the set of constraints (8) may be satisfied by various routing variables T_{ij} . Introducing a strictly concave objective function $V_{ij}(T_{ij})$ associated with the variable T_{ij} , we can ensure uniqueness of the variables T_{ij} . Incorporating such

an objective function and the routing constraints (8) in the optimization problem (4), we obtain the following constrained coverage problem:

$$\begin{aligned} & \underset{\mathbf{x}, \mathbf{t}, \mathcal{W}}{\text{maximize}} && \mathcal{H}(\mathbf{x}, \mathcal{W}) + \sum_{i=1}^N \sum_{j=1}^{N+K} V_{ij}(T_{ij}) && (9) \\ & \text{subject to} && c_i(\mathbf{x}_i, \mathcal{W}_i, \mathbf{t}) \geq 0 \\ & && \sum_{j=1}^{N+K} T_{ij} \leq 1, \quad 0 \leq T_{ij} \leq 1, \quad \forall j \end{aligned}$$

where the constraints in (9) hold for all robots $i \in \{1, \dots, N\}$. In (9), we have also introduced the constraint $0 \leq T_{ij} \leq 1$, since the variables T_{ij} represent fractions of time, as well as the constraint $\sum_{j=1}^{N+K} T_{ij} \leq 1$, which ensures that the sum of time shares at node i does not exceed 1. Finally for the strictly concave objective functions V_{ij} , we select $V_{ij} = -w_{ij}T_{ij}^2$, $w_{ij} > 0$ in order to encourage packet splitting over different paths increasing in this way the robustness to link failures.

In the absence of the constraints, it is well known that the objective function \mathcal{H} in (9) is maximized if the partition \mathcal{W}_i is chosen to be the Voronoi partition of the space; see Proposition 2.13 in [32]; defined as:

Definition 1 ([33]) *The Voronoi diagram generated by a set of points located at $\{\mathbf{x}_1, \dots, \mathbf{x}_N\}$, is the set $\mathcal{V} = \{\mathcal{V}_1, \dots, \mathcal{V}_N\}$ where \mathcal{V}_i is called the Voronoi cell of node i and contains the points that are closer to it than to any other node:*

$$\mathcal{V}_i = \{\mathbf{q} \in \mathcal{A} \mid \|\mathbf{q} - \mathbf{x}_i\| \leq \|\mathbf{q} - \mathbf{x}_j\|, \quad \forall j \neq i\}.$$

On the other hand, in the presence of the constraints, the Voronoi regions are not necessarily feasible for (9) and, therefore, the feasible optimal partition for the constrained problem (9) is in general different from the Voronoi partition. However, if we are able to ensure feasibility of the Voronoi partition, then this partition will be optimal for (9). In our problem, this is possible by appropriately selecting the routing probabilities T_{ij} . In particular, we replace the partition \mathcal{W} in (9) by the Voronoi partition \mathcal{V} , and then solve for routes T_{ij} that satisfy the constraints. This gives rise to the following problem:

$$\begin{aligned} & \underset{\mathbf{x}, \mathbf{t}}{\text{maximize}} && \left[P(\mathbf{x}, \mathbf{t}) = \mathcal{H}(\mathbf{x}) + \sum_{i=1}^N \sum_{j=1}^{N+K} V_{ij}(T_{ij}) \right] && (10) \\ & \text{subject to} && c_i(\mathbf{x}, \mathbf{t}) \geq 0 \\ & && \sum_{j=1}^{N+K} T_{ij} \leq 1, \quad 0 \leq T_{ij} \leq 1, \quad \forall j \end{aligned}$$

where again the constraints in (10) hold for all robots $i \in \{1, \dots, N\}$. Comparing to (4) and (8), in (10) we have dropped the dependence of the objective \mathcal{H} and the constraints c_i on the Voronoi partition \mathcal{V} . The reason is that, unlike any arbitrary partition \mathcal{W} , the Voronoi partition is completely determined by the robot positions \mathbf{x} . Note also that for the computation of the rate $r_i(\mathbf{x})$ in the constraint $c_i(\mathbf{x}, \mathbf{t}) \geq 0$ only information acquired by the set of Delaunay neighbors denoted by \mathcal{D}_i is required, where $\mathcal{D}_i = \{j \neq i \mid V_i \cap V_j \neq \emptyset \text{ (non-singleton)}\}$. Note that for a fixed spatial configuration of the robots \mathbf{x} , the reliabilities $R(\mathbf{x}_i, \mathbf{x}_j)$ are fixed and, therefore, the problem in (10) attains a simple concave form. Throughout the rest of the paper, we assume that the optimization problem in (10) is initially feasible given the initial network configuration, i.e., that paths exist that can support the desired rates of information between all nodes and the access points. This can be achieved by, e.g., starting at a configuration at which all robots are close to the APs.

3 Distributed Optimal Communication

A centralized solution of (10), as in [2], can incur large communication cost and delays due to the need of identifying the network topology and communicating it to all robots. Therefore, a distributed solution is preferred, where (10) is solved locally across the group of nodes. In particular, given fixed robot positions \mathbf{x} and following the steps of [22], we define the Lagrangian of (10) as¹

$$\begin{aligned} \mathcal{L}_{\mathbf{x}}(\boldsymbol{\lambda}, \mathbf{t}) &= \sum_{i=1}^N \sum_{j=1}^{N+K} V_{ij}(T_{ij}) && (11) \\ &+ \sum_{i=1}^N \boldsymbol{\lambda}_i \left[\sum_{j=1}^{N+K} T_{ij} R(\mathbf{x}_i, \mathbf{x}_j) - \sum_{j=1}^N T_{ji} R(\mathbf{x}_j, \mathbf{x}_i) - r_i(\mathbf{x}) \right], \end{aligned}$$

where $\boldsymbol{\lambda} \in \mathbb{R}^N$ is a column vector of the Lagrange multipliers. Then the dual function is defined as

$$g_{\mathbf{x}}(\boldsymbol{\lambda}) = \max_{\sum_{j=1}^{N+K} T_{ij} \leq 1, \forall i \in \{1, \dots, N\}} \mathcal{L}_{\mathbf{x}}(\boldsymbol{\lambda}, \mathbf{t}). \quad (12)$$

and the dual problem becomes

$$D_{\mathbf{x}} = \min_{\boldsymbol{\lambda} \geq 0} g_{\mathbf{x}}(\boldsymbol{\lambda}).$$

Since for a fixed spatial configuration \mathbf{x} the problem in (10) is concave, it holds that $P_{\mathbf{x}} = D_{\mathbf{x}}$, where $P_{\mathbf{x}}$ is the solution of (10) for fixed \mathbf{x} . Therefore, we can equivalently work with the dual problem.

¹ Since we assume fixed robot positions \mathbf{x} , the term $\mathcal{H}(\mathbf{x})$ in the objective function of (10) is a constant; therefore, for the sake of simplicity, in the construction of the Lagrangian, it can be ignored.

To implement a gradient descent algorithm in the dual domain, we need to define first the primal Lagrangian maximizers as:

$$\{T_{\mathbf{x},ij}(\boldsymbol{\lambda})\}_{\forall i,j} = \operatorname{argmax}_{\sum_{j=1}^{N+K} T_{ij} \leq 1} \mathcal{L}_{\mathbf{x}}(\boldsymbol{\lambda}, \mathbf{t}). \quad (13)$$

Then, the i -th component of the gradient of the dual function (12) is given by:

$$\begin{aligned} [\nabla g_{\mathbf{x}}(\boldsymbol{\lambda})]_i &= \sum_{j=1}^{N+K} T_{\mathbf{x},ij} R(\mathbf{x}_i, \mathbf{x}_j) \\ &\quad - \sum_{j=1}^N T_{\mathbf{x},ji} R(\mathbf{x}_j, \mathbf{x}_i) - r_i(\mathbf{x}). \end{aligned} \quad (14)$$

Note that the Lagrangian defined in (11) can be expressed as a sum of local Lagrangians $\mathcal{L}_{\mathbf{x},i}$ through reordering its terms, which depend only on variables $\{T_{ij}\}_{j=1}^N$, i.e.,

$$\mathcal{L}_{\mathbf{x}}(\boldsymbol{\lambda}, \mathbf{t}) = \sum_{i=1}^N \mathcal{L}_{\mathbf{x},i}(\boldsymbol{\lambda}, \mathbf{t}),$$

where

$$\begin{aligned} \mathcal{L}_{\mathbf{x},i}(\boldsymbol{\lambda}, \mathbf{t}) &= -\lambda_i r_i(\mathbf{x}) \\ &\quad + \sum_{j=1}^N [V_{ij}(T_{ij}) + T_{ij} R(\mathbf{x}_i, \mathbf{x}_j)(\lambda_i - \lambda_j)] \\ &\quad + \sum_{j=N+1}^{N+K} [V_{ij}(T_{ij}) + \lambda_i T_{ij} R(\mathbf{x}_i, \mathbf{x}_j)]. \end{aligned} \quad (15)$$

Since the variables $\{T_{ij}\}_{j=1}^N$ appear only in $\mathcal{L}_{\mathbf{x},i}$, finding the primal variables that maximize the global Lagrangian is equivalent to computing the maximizers of the local Lagrangians in (15),

$$\{T_{\mathbf{x},ij}(\boldsymbol{\lambda})\}_{j=1}^{N+K} = \operatorname{argmax}_{\sum_{j=1}^{N+K} T_{ij} \leq 1} \mathcal{L}_{\mathbf{x},i}(\boldsymbol{\lambda}, \mathbf{t}). \quad (16)$$

Introducing finally an index k and denoting by t_k the time instants at which the variables are updated, we can write the following distributed gradient descent algorithm in the dual domain:

Primal Iteration For a given spatial configuration $\mathbf{x}(t_k)$ and Lagrange multipliers $\boldsymbol{\lambda}(t_k)$, compute Lagrangian maximizers $\{T_{\mathbf{x}(t_k),ij}\}_{j=1}^{N+K}$ according to (16) as:

$$\{T_{\mathbf{x},ij}(t_k)\}_{j=1}^{N+K} = \operatorname{argmax}_{\sum_{j=1}^{N+K} T_{ij} \leq 1} \mathcal{L}_{\mathbf{x}(t_k),i}(\boldsymbol{\lambda}(t_k), \mathbf{t}). \quad (17)$$

Dual Iteration Given the primal variables $\{T_{\mathbf{x},ij}(t_k)\}_{j=1}^{N+K}$ from (17), update the dual variables as:

$$\begin{aligned} \lambda_i(t_{k+1}) &= \mathbb{P} \left[\lambda_i(t_k) - \epsilon \left(\sum_{j=1}^{N+K} T_{ij}(t_k) R(\mathbf{x}_i(t_k), \mathbf{x}_j(t_k)) \right. \right. \\ &\quad \left. \left. - \sum_{j=1}^N T_{ji}(t_k) R(\mathbf{x}_j(t_k), \mathbf{x}_i(t_k)) - r_i(\mathbf{x}) \right) \right], \end{aligned} \quad (18)$$

where \mathbb{P} denotes the projection to the non-negative orthant. Note, that the algorithm (17)-(18) is distributed, since it requires only the Lagrange multipliers λ_j (equation (17)) and the routing variables T_{ji} (equation (18)) from robots for which $R_{ij} \neq 0$. In the next section, we integrate communication control with robot mobility for area coverage maximization.

Remark 2 (Primal-Dual Decomposition) *In the above analysis, the dual subgradient method [34] was implemented in order to compute the optimal routing decisions T_{ij} for a given network configuration \mathbf{x} . More sophisticated primal-dual decomposition algorithms, e.g., the Alternating Direction Method of Multipliers (ADMM) [35], or the Accelerated Distributed Augmented Lagrangian (ADAL) [36], can also be used in lieu of the existing one, which enjoy faster convergence rates.*

4 Simultaneous Coverage and Routing Control

To jointly optimize coverage and communication we propose a hybrid scheme that decouples the two control objectives and alternates between optimization of the two. Specifically, at each time instant t_k , the routing variables are updated via the distributed algorithm (17)-(18) and during the time intervals (t_k, t_{k+1}) the robots move towards configurations $\mathbf{x}_i(t_{k+1})$ that optimize coverage. Since the update (17)-(18) ensures feasibility of the primal variables for a static network as $k \rightarrow \infty$, for any finite k and a mobile network, the primal variables $\{T_{ij}\}_{j=1}^{N+K}$ are not necessarily feasible. This means that the communication constraint $c_i(\mathbf{x}(t), \mathbf{t}) \geq 0$ may become violated as the i -th robot moves from $\mathbf{x}_i(t_k)$ to $\mathbf{x}_i(t_{k+1})$. To ensure that this constraint violation does not grow large and, therefore, that an acceptable quality of communication is maintained, every robot needs to check feasibility of its local routing variables after every communication update. Robots for which these routing variables are infeasible remain stationary until the iteration (17)-(18) returns feasible routes. When feasible routes are obtained, those robots compute their next position $\mathbf{x}_i(t_{k+1})$ and start moving towards it.

To ensure that robot motion is free of collisions between robots or between robots and the workspace boundary, we introduce additional collision avoidance constraints

that the robots need to respect as they move to optimize coverage. Specifically, for every time t_k , we restrict the feasible space for the next position $\mathbf{x}_i(t_{k+1})$ of every robot i to be in the associated Voronoi cell $\mathcal{V}_i(t_k)$ excluding its boundary $\partial\mathcal{V}_i(t_k)$. Since the Voronoi cells are disjoint sets, except at their boundary, this constraint will prevent any two robots from simultaneously colliding at any common point $\mathbf{q} \in \mathcal{A}$. To construct this collision avoidance constraint note that any Voronoi cell \mathcal{V}_i can be expressed by the intersection of half-spaces that include \mathbf{x}_i as

$$\mathcal{V}_i(t_k) = \bigcap_{e=1}^{E_i(t_k)} \{\mathbf{q} \mid \mathbf{a}_e^i(t_k)^T \mathbf{q} \leq b_e^i(t_k)\}, \quad (19)$$

where $E_i(t_k)$ is the number of edges that constitute $\partial\mathcal{V}_i(t_k)$. Then, the feasible space for robot i at time t_k can be defined as

$$\mathcal{F}_i(t_k) = \bigcap_{e=1}^{E_i(t_k)} \{\mathbf{q} \mid \mathbf{a}_e^i(t_k)^T \mathbf{q} \leq b_e^i(t_k) + \rho_e^i(t_k)\}, \quad (20)$$

where $\rho_e^i(t_k)$ are constants used to translate the half-spaces that constitute the Voronoi cell $\mathcal{V}_i(t_k)$ so that for every e , the distance between the lines $\mathbf{a}_e^i(t_k)^T \mathbf{q} = b_e^i(t_k)$ and $\mathbf{a}_e^i(t_k)^T \mathbf{q} = b_e^i(t_k) + \rho_e^i(t_k)$ is equal to $\rho > 0$ and $\mathcal{F}_i(t_k) \subset \mathcal{V}_i(t_k)$. Then, requiring that $\mathbf{x}_i(t_{k+1}) \in \mathcal{F}_i(t_k)$ ensures collision avoidance among the robots, since the inter-robot distance will be always greater than or equal to $2\rho > 0$. Expressing all constraints in (20) in vector form, we can equivalently write $\mathbf{x}_i \in \mathcal{F}_i(t_k)$ as

$$\mathbf{g}_i(\mathbf{x}_i, \mathbf{x}(t_k)) = \mathbf{b}_i(\mathbf{x}(t_k)) - \mathbf{A}_i(\mathbf{x}(t_k))\mathbf{x}_i \geq \mathbf{0}. \quad (21)$$

Note that constructing the constraint in (21) requires only information acquired by the set of Delaunay neighbors of robot i . The feasible spaces that guarantee collision avoidance for a simple network of three robots is depicted in Figure 1.

Using the above construction, motion planning is via the solution of local sequential concave programs that allow to handle the nonlinear dependence of the constraints and coverage objective in the optimization problem (10) on the robot positions. In particular, assuming that all other robots are fixed at positions $\mathbf{x}_j(t_k)$ for $j \neq i$ and given routing decisions $\mathbf{t}(t_k)$, every robot i solves the following problem:

$$\begin{aligned} & \underset{\mathbf{x}_i}{\text{maximize}} \quad \tilde{\mathcal{H}}(\mathbf{x}_i, \mathbf{x}(t_k)) & (22) \\ & \text{subject to} \quad \tilde{c}_i(\mathbf{x}_i, \mathbf{x}(t_k), \mathbf{t}(t_k)) \geq 0, \\ & \quad \|\mathbf{x}_i - \mathbf{x}_i(t_k)\| \leq \sigma, \\ & \quad \mathbf{g}_i(\mathbf{x}_i, \mathbf{x}(t_k)) \geq \mathbf{0}, \end{aligned}$$

for the next position $\mathbf{x}_i(t_{k+1})$, where $\tilde{\mathcal{H}}$ and \tilde{c}_i are a concave and linear approximation of c_i and \mathcal{H} , respectively,

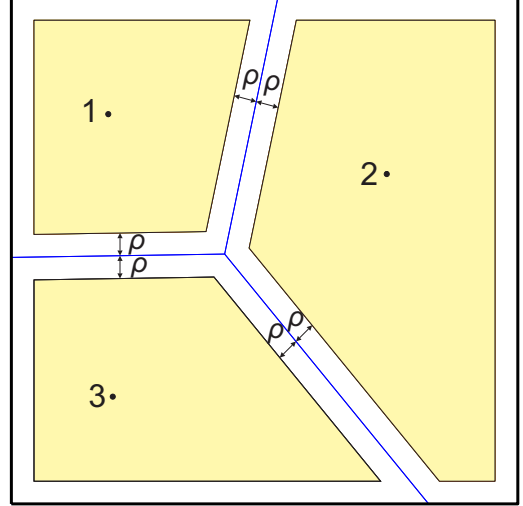


Fig. 1. Graphical example of the feasible sets that guarantee collision avoidance for a network of three robots. Blue lines determine the Voronoi cells for each robot and the yellow colored polygonal areas stand for the sets \mathcal{F}_i as defined in (20).

i.e.,

$$\begin{aligned} \tilde{c}_i(\mathbf{x}_i, \mathbf{x}(t_k), \mathbf{t}(t_k)) &= & (23) \\ &= c_i(\mathbf{x}(t_k), \mathbf{t}(t_k)) + (\nabla_{\mathbf{x}_i} c_i(\mathbf{x}(t_k), \mathbf{t}(t_k)))^T (\mathbf{x}_i - \mathbf{x}_i(t_k)), \end{aligned}$$

and

$$\begin{aligned} \tilde{\mathcal{H}}(\mathbf{x}_i, \mathbf{x}(t_k)) &= & (24) \\ &= \mathcal{H}(\mathbf{x}(t_k)) + (\nabla_{\mathbf{x}_i} \mathcal{H}(\mathbf{x}(t_k)))^T (\mathbf{x}_i - \mathbf{x}_i(t_k)) \\ & \quad + (\mathbf{x}_i - \mathbf{x}_i(t_k))^T \mathbf{H}^k(\mathbf{x}_i - \mathbf{x}_i(t_k)), \end{aligned}$$

where \mathbf{H}^k stands for a negative definite approximation of the Hessian of $\mathcal{H}(\mathbf{x})$ evaluated at $\mathbf{x}(t_k)$, which can be obtained with known techniques, such as the Broyden-Fletcher-Goldfarb-Shanno method (BFGS) [37] that only requires the gradient of \mathcal{H} . The distributed computation of the gradient of the coverage objective \mathcal{H} will be shown in Proposition 6. In the proposed sequential concave program (22), $\sigma > 0$ denotes a trust region where the concave and linear models in (23) and (24) are adequate approximations of the coverage objective and the communication constraint, respectively. Assuming that the maximum robot speed is absolutely bounded as

$$\max_i \|\dot{\mathbf{x}}_i\| \leq \alpha, \quad (25)$$

for some constant $0 < \alpha < \infty$ and letting $\Delta t = \max_k \{t_{k+1} - t_k\}$, the trust region must satisfy $\sigma \leq \alpha \Delta t$.

Rewriting (1) in discrete time and letting $\mathbf{x}_i(t_{k+1})$ be the solution of (22), we obtain the controller for the i -th

Algorithm 1 Simultaneous coverage and routing control at robot i

- 1: **for** $k = 0$ to ∞ **do**
 - 2: Compute the routing probabilities $\{T_{ij}\}_{j=1}^{N+K}$ via the primal-dual algorithm (17)-(18);
 - 3: **if** $c_i(\mathbf{x}(t_k), \mathbf{t}) \geq 0$ **then**
 - 4: Compute next position $\mathbf{x}_i(t_{k+1})$ via the optimization problem (22);
 - 5: Move towards $\mathbf{x}_i(t_{k+1})$ according to (26);
 - 6: **else**
 - 7: Stay motionless;
 - 8: **end if**
 - 9: **end for**
-

robot as

$$\mathbf{u}_i(t) = \frac{\mathbf{x}_i(t_{k+1}) - \mathbf{x}_i(t_k)}{\Delta t}, \quad \forall t \in (t_k, t_{k+1}). \quad (26)$$

The aforementioned control scheme is also summarized for the i -th robot, in Algorithm 1.

Remark 3 (Voronoi cells) *The distributed evaluation of the i -th Voronoi cell in (23) can be achieved via the algorithm presented in [3].*

Remark 4 (Hessian) *Computation of the Hessian in (24) requires only local information as the term $\mathcal{H}(\mathbf{x}(t_k))$ does not include the variable $\mathbf{x}_i(t_{k+1})$ and, therefore, it does not affect the optimization in (22).*

Remark 5 (Computational Cost) *At every iteration, every robot computes the routing decisions via the primal-dual algorithm (17)-(18) and the updated position $\mathbf{x}_i(t_{k+1})$ via the solution of the optimization problem (22). Note that (17) and (22) are constrained, strictly convex, quadratic programs which can be solved in polynomial time using standard techniques [38].*

4.1 Distributed Gradient Results

Observe that equations (23) and (24) require the gradients $\nabla_{\mathbf{x}_i} \mathcal{H}$ and $\nabla_{\mathbf{x}_i} r_i$, respectively. Since the positions of the robots can never coincide due to the collision avoidance constraint $\mathbf{g}_i(\mathbf{x}_i, \mathbf{x}(t_k)) \geq \mathbf{0}$, the reformulation of the coverage objective in (4) is valid and it is also differentiable according to Theorem 2.2 in [4]. Therefore, the existence of the gradient $\nabla_{\mathbf{x}_i} \mathcal{H}(\mathbf{x})$ is guaranteed for all time t . To obtain the gradients $\nabla_{\mathbf{x}_i} \mathcal{H}$ and $\nabla_{\mathbf{x}_i} r_i$ we show the following results:

Proposition 6 *Given the differentiable function f defined in (2), a density function ϕ , and the Voronoi partitioning of an area of interest \mathcal{A} , the gradient of the coverage objective defined in (4) can be expressed as follows:*

$$\nabla_{\mathbf{x}_i} \mathcal{H}(\mathbf{x}) = 2 \int_{\mathcal{V}_i} (\mathbf{q} - \mathbf{x}_i) e^{-\|\mathbf{q} - \mathbf{x}_i\|^2} \phi(\mathbf{q}) d\mathbf{q}. \quad (27)$$

PROOF. Applying Theorem 2.2 of [4] and considering that the function f defined in (2) is continuous, we have

$$\begin{aligned} \nabla_{\mathbf{x}_i} \mathcal{H}(\mathbf{x}) &= \int_{\mathcal{V}_i} \frac{\partial f(\mathbf{x}_i, \mathbf{q})}{\partial \mathbf{x}_i} \phi(\mathbf{q}) d\mathbf{q} \\ &= 2 \int_{\mathcal{V}_i} (\mathbf{q} - \mathbf{x}_i) e^{-\|\mathbf{q} - \mathbf{x}_i\|^2} \phi(\mathbf{q}) d\mathbf{q}, \end{aligned} \quad (28)$$

completing the proof. \square

Proposition 7 *Given a differentiable function f and a density function ϕ , the gradient of the function r_i defined in (5) can be expressed as follows:*

$$\begin{aligned} \nabla_{\mathbf{x}_i} r_i(\mathbf{x}) &= \int_{\mathcal{V}_i} \frac{\partial f(\mathbf{q}, \mathbf{x}_i)}{\partial \mathbf{x}_i} \phi(\mathbf{q}) d\mathbf{q} \\ &+ \sum_{j=1}^{d_i} \int_{\partial \mathcal{V}_i \cap \partial \mathcal{V}_j} \frac{\mathbf{q} - \mathbf{x}_i}{\|\mathbf{x}_j - \mathbf{x}_i\|} f(\mathbf{q}, \mathbf{x}_i) \phi(\mathbf{q}) d\mathbf{q}, \end{aligned} \quad (29)$$

where $\partial \mathcal{V}_i$ stands for the polygonal boundary of the Voronoi cell \mathcal{V}_i and d_i is the number of Delaunay neighbors of robot i .

PROOF. The first steps of the proof are conceptually similar to the proofs presented in [4, 10, 13]. Applying the Leibniz integral rule [39] to the expression for r_i in (5), we have:

$$\begin{aligned} \nabla_{\mathbf{x}_i} r_i &= \frac{\partial}{\partial \mathbf{x}_i} \int_{\mathcal{V}_i} f(\mathbf{q}, \mathbf{x}_i) \phi(\mathbf{q}) d\mathbf{q} \\ &= \int_{\mathcal{V}_i} \frac{\partial f(\mathbf{q}, \mathbf{x}_i)}{\partial \mathbf{x}_i} \phi(\mathbf{q}) d\mathbf{q} + \int_{\partial \mathcal{V}_i} \mathbf{n}_i^T \frac{\partial \mathbf{q}}{\partial \mathbf{x}_i} f(\mathbf{q}, \mathbf{x}_i) \phi(\mathbf{q}) d\mathbf{q}, \end{aligned} \quad (30)$$

where \mathbf{n}_i is the normal unit vector pointing outwards of an edge of the Voronoi cell \mathcal{V}_i .

Looking at the second integral of (30), we can decompose the polygonal boundary $\partial \mathcal{V}_i$ into edges that lie in either $\partial \mathcal{A}$ or $\partial \mathcal{V}_i \cap \partial \mathcal{V}_j$, $\forall j \in \mathcal{D}_i$. Therefore, we can rewrite (30) as follows:

$$\begin{aligned} \nabla_{\mathbf{x}_i} r_i &= \int_{\mathcal{V}_i} \frac{\partial f(\mathbf{q}, \mathbf{x}_i)}{\partial \mathbf{x}_i} \phi(\mathbf{q}) d\mathbf{q} \\ &+ \sum_{j=1}^{d_i} \int_{\partial \mathcal{V}_i \cap \partial \mathcal{V}_j} \mathbf{n}_i^T \frac{\partial \mathbf{q}}{\partial \mathbf{x}_i} f(\mathbf{q}, \mathbf{x}_i) \phi(\mathbf{q}) d\mathbf{q} \\ &+ \int_{\partial \mathcal{V}_i \cap \partial \mathcal{A}} \mathbf{n}_i^T \frac{\partial \mathbf{q}}{\partial \mathbf{x}_i} f(\mathbf{q}, \mathbf{x}_i) \phi(\mathbf{q}) d\mathbf{q}. \end{aligned} \quad (31)$$

Since the points $\mathbf{q} \in \partial \mathcal{A}$ are not affected by the robots' motion, we have that $\frac{\partial \mathbf{q}}{\partial \mathbf{x}_i} = \mathbf{0}$ for all $\mathbf{q} \in \partial \mathcal{V}_i \cap \partial \mathcal{A}$. Consequently, the third term in (31) is zero. As for the

second term, observe that the vector \mathbf{n}_i at points $\mathbf{q} \in \partial\mathcal{V}_i \cap \partial\mathcal{V}_j$, for some $j \in \mathcal{D}_i$, can be expressed as:

$$\mathbf{n}_i = \frac{\mathbf{x}_j - \mathbf{x}_i}{\|\mathbf{x}_j - \mathbf{x}_i\|}.$$

These points $\mathbf{q} \in \partial\mathcal{V}_i \cap \partial\mathcal{V}_j$ lie on the line described by the equation:

$$\mathbf{q} = \frac{\mathbf{x}_i + \mathbf{x}_j}{2} + a_{ij} \mathbf{C}_{ij} (\mathbf{x}_j - \mathbf{x}_i), \quad (32)$$

where \mathbf{C}_{ij} is the skew symmetric rotation matrix

$$\mathbf{C}_{ij} = \begin{bmatrix} 0 & -1 \\ 1 & 0 \end{bmatrix},$$

so that $\mathbf{C}_{ij}(\mathbf{x}_j - \mathbf{x}_i)$ is perpendicular to $(\mathbf{x}_j - \mathbf{x}_i)$, and $a_{ij} \in \mathbb{R}$ is a scalar. Taking the partial derivative of (32) with respect to \mathbf{x}_i yields:

$$\frac{\partial \mathbf{q}}{\partial \mathbf{x}_i} = \frac{1}{2} \mathbf{I} - a_{ij} \mathbf{C}_{ij}, \quad (33)$$

where \mathbf{I} stands for the identity matrix. Multiplying (33) from the left by \mathbf{n}_i^T , we have:

$$\begin{aligned} \mathbf{n}_i^T \frac{\partial \mathbf{q}}{\partial \mathbf{x}_i} &= \frac{1}{2} \mathbf{n}_i^T - a_{ij} \mathbf{n}_i^T \mathbf{C}_{ij} \\ &= \frac{1}{2} \frac{(\mathbf{x}_j - \mathbf{x}_i)^T}{\|\mathbf{x}_j - \mathbf{x}_i\|} + a_{ij} \frac{(\mathbf{x}_j - \mathbf{x}_i)^T}{\|\mathbf{x}_j - \mathbf{x}_i\|} \mathbf{C}_{ij}^T \\ &= \frac{1}{2} \frac{(\mathbf{x}_j - \mathbf{x}_i)^T}{\|\mathbf{x}_j - \mathbf{x}_i\|} + \frac{1}{\|\mathbf{x}_j - \mathbf{x}_i\|} \left(\mathbf{q}^T - \frac{(\mathbf{x}_i + \mathbf{x}_j)^T}{2} \right) \\ &= \frac{\mathbf{q}^T - \mathbf{x}_i^T}{\|\mathbf{x}_j - \mathbf{x}_i\|}, \end{aligned} \quad (34)$$

where in the third equality of (34), we have substituted the term $a_{ij}(\mathbf{x}_j - \mathbf{x}_i)^T \mathbf{C}_{ij}^T$ from (32).

Substituting equation (34) into (30) yields:

$$\begin{aligned} \nabla_{\mathbf{x}_i} r_i &= \int_{\mathcal{V}_i} \frac{\partial f(\mathbf{q}, \mathbf{x}_i)}{\partial \mathbf{x}_i} \phi(\mathbf{q}) d\mathbf{q} \\ &\quad + \sum_{j=1}^{d_i} \int_{\partial\mathcal{V}_i \cap \partial\mathcal{V}_j} \frac{\mathbf{q} - \mathbf{x}_i}{\|\mathbf{x}_j - \mathbf{x}_i\|} f(\mathbf{q}, \mathbf{x}_i) \phi(\mathbf{q}) d\mathbf{q}, \end{aligned} \quad (35)$$

completing the proof of the proposition. \square

5 Algorithm Analysis

As discussed in Section 4, robot mobility can cause persistent infeasibility gaps in the communication con-

straints in problem (10). Additional constraint violations can enter the system due to the convex approximations of the constraints c_i in the sequential convex programs (22) that are solved for motion planning. Specifically, in this latter case, violations of the communication constraints (8) can be introduced, since (22) can return updated robot positions $\mathbf{x}_i(t_k + 1)$ that might not necessarily satisfy the original nonlinear communication constraint c_i . In this section, we obtain bounds on problem specific parameters that result in bounded violations of the communication constraints (8), so that a desired performance of communications is maintained. In particular, we show how to select the trust region $\sigma > 0$, robot speed $\alpha > 0$, and time intervals $\Delta t = \max_k \{t_{k+1} - t_k\}$ so that the information collected by the mobile sensors can be reliably transmitted to the APs, as per equation (8).

Throughout the rest of the paper, to simplify notation we write the constraints in (8) as $\mathbf{A}_x \mathbf{t} - \mathbf{r}_x \geq 0$, where $\mathbf{A}_x \in \mathbb{R}^{N \times N(N+K)}$ is a matrix containing the channel reliabilities $R(\mathbf{x}_i, \mathbf{x}_j)$ between adjacent robots, $\mathbf{t} \in \mathbb{R}^{N(N+K)}$ is vector that stacks the routing decisions of all robots, and $\mathbf{r}_x \in \mathbb{R}^N$ is a vector containing the transmission rates for all robots. Using this notation, the dual function defined in (12) can be equivalently written as

$$g_x(\boldsymbol{\lambda}) = \max_{\mathbf{t}} \left\{ f_0(\mathbf{t}(\boldsymbol{\lambda})) + \boldsymbol{\lambda}^T [\mathbf{A}_x \mathbf{t} - \mathbf{r}_x] \right\}. \quad (36)$$

In what follows, we adopt an analysis similar to [22], which requires the following assumptions:

- (a) The dual functions $g_x(\boldsymbol{\lambda})$ are strongly convex for all \mathbf{x} with common strong convexity parameter m ,

$$g_x(\boldsymbol{\mu}) \geq g_x(\boldsymbol{\lambda}) + \nabla g_x(\boldsymbol{\lambda}) + \frac{m}{2} \|\boldsymbol{\lambda} - \boldsymbol{\mu}\|^2. \quad (37)$$

- (b) The gradients of the dual function are Lipschitz continuous with common Lipschitz constant M .
- (c) The 2-norm of the dual gradients $\nabla g_x(\boldsymbol{\lambda})$ are uniformly bounded for all $\boldsymbol{\lambda}$ and \mathbf{x} .
- (d) The 1-norm of the optimal Lagrange multipliers $\boldsymbol{\lambda}_x^*$ are uniformly bounded for all \mathbf{x} .

$$\|\boldsymbol{\lambda}_x^*\|_1 \leq \lambda_{\max}. \quad (38)$$

These assumptions are mild and commonly used in analysis of gradient descent algorithms, e.g., in [22]. The dual function is strongly convex as required by Assumption (a) if the objective functions V_{ij} have Lipschitz gradients and the matrix $\mathbf{A}_x \mathbf{A}_x^T$ is full row rank. Also, for the problem under consideration, Assumption (b) holds, since the selected objective functions $V_{ij} = -w_{ij} T_{ij}^2$ are strongly convex. Moreover, the bound G_{\max} in Assumption (c) exists, since the dual gradients are given by the constraint violations as per (14) and the primal variables

T_{ij} are finite. The bound on the optimal dual variables assumed in Assumption (d) exists provided the existence of a strictly feasible solution of (10) for a fixed \mathbf{x} is guaranteed.

The following proposition describes how to choose the trust-region size σ , the robot speed α and the time interval Δt , so that the channel reliabilities and the average rates of information generated at the sensors at subsequent iterations are absolutely bounded.

Proposition 8 *Assume symmetric channel reliabilities so that $R(\mathbf{x}_i, \mathbf{x}_j) = R(\mathbf{x}_j, \mathbf{x}_i)$ and assume also that the gradients $\nabla_{\mathbf{x}_i} R(\mathbf{x}_i, \mathbf{x}_j)$ and $\nabla_{\mathbf{x}_i} \mathbf{r}_i$ are absolutely bounded by M_R and M_r , respectively, i.e.,*

$$\max_i \|\nabla_{\mathbf{x}_i} R(\mathbf{x}_i, \mathbf{x}_j)\| \leq M_R < \infty, \quad (39)$$

and

$$\max_{i,j} \|\nabla_{\mathbf{x}_j} \mathbf{r}_{\mathbf{x},i}\| \leq M_r < \infty. \quad (40)$$

Then, for any constants $\delta > 0$ and $\gamma > 0$, choosing the trust region $\sigma > 0$, robot speed $\alpha > 0$ in (25), and the time interval $\Delta t = \max_k \{t_{k+1} - t_k\}$ such that

$$\sigma \leq \alpha \Delta t \leq \min \left\{ \frac{\delta}{2M_R}, \frac{\gamma}{NM_r} \right\}, \quad (41)$$

ensures that the channel reliabilities and the average rates of information generated at the sensors at subsequent iterations are absolutely bounded as

$$|R(\mathbf{x}_i(t_{k+1}), \mathbf{x}_j(t_{k+1})) - R(\mathbf{x}_i(t_k), \mathbf{x}_j(t_k))| \leq \delta, \quad (42)$$

and

$$|\mathbf{r}_{\mathbf{x}(t_{k+1}),i} - \mathbf{r}_{\mathbf{x}(t_k),i}| \leq \gamma. \quad (43)$$

PROOF. Note first that the existence of finite upper bounds M_R and M_r in (39) and (40) is ensured by the fact that robot motion is restricted within a bounded trust-region $\sigma > 0$ and since the Voronoi cells are bounded sets due to boundedness of the area \mathcal{A} . To show this result, we need to associate the bounds $\delta > 0$ and $\gamma > 0$ on the rates of change of the functions $R(\mathbf{x}_i(t), \mathbf{x}_j(t))$ and $\mathbf{r}_{\mathbf{x},i}$, respectively, with the trust region $\sigma > 0$. We begin by looking at the reliabilities $R(\mathbf{x}_i(t), \mathbf{x}_j(t))$. Observe that for all time t we have

$$\begin{aligned} \dot{R}(\mathbf{x}_i(t), \mathbf{x}_j(t)) &= \\ &= \nabla_{\mathbf{x}_i} R(\mathbf{x}_i(t), \mathbf{x}_j(t)) \dot{\mathbf{x}}_i + \nabla_{\mathbf{x}_j} R(\mathbf{x}_i(t), \mathbf{x}_j(t)) \dot{\mathbf{x}}_j \\ &= \nabla_{\mathbf{x}_i} R(\mathbf{x}_i(t), \mathbf{x}_j(t)) (\dot{\mathbf{x}}_i - \dot{\mathbf{x}}_j), \end{aligned} \quad (44)$$

where in the last equality follows from the fact that $\nabla_{\mathbf{x}_i} R(\mathbf{x}_i(t), \mathbf{x}_j(t)) = -\nabla_{\mathbf{x}_j} R(\mathbf{x}_i(t), \mathbf{x}_j(t))$, for symmetric channel reliabilities that satisfy $R(\mathbf{x}_i, \mathbf{x}_j) =$

$R(\mathbf{x}_j, \mathbf{x}_i)$. Taking the absolute value of (44) gives

$$\begin{aligned} |\dot{R}(\mathbf{x}_i(t), \mathbf{x}_j(t))| &= |\nabla_{\mathbf{x}_i} R(\mathbf{x}_i(t), \mathbf{x}_j(t)) (\dot{\mathbf{x}}_i - \dot{\mathbf{x}}_j)| \\ &\leq \|\nabla_{\mathbf{x}_i} R(\mathbf{x}_i(t), \mathbf{x}_j(t))\| (\|\dot{\mathbf{x}}_i\| + \|\dot{\mathbf{x}}_j\|) \\ &\leq 2M_R \alpha, \end{aligned} \quad (45)$$

where the last inequality is due to the bounds in (39) and (25).

Expressing the quantity $|R(\mathbf{x}_i(t_k + \Delta t), \mathbf{x}_j(t_k + \Delta t)) - R(\mathbf{x}_i(t_k), \mathbf{x}_j(t_k))|$ as a definite integral, we have that

$$\begin{aligned} |R(\mathbf{x}_i(t_k + \Delta t), \mathbf{x}_j(t_k + \Delta t)) - R(\mathbf{x}_i(t_k), \mathbf{x}_j(t_k))| &= \\ &= \left| \int_{t_k}^{t_k + \Delta t} \dot{R}(\mathbf{x}_i(\tau), \mathbf{x}_j(\tau)) d\tau \right| \leq \\ &\leq \int_{t_k}^{t_k + \Delta t} |\dot{R}(\mathbf{x}_i(\tau), \mathbf{x}_j(\tau))| d\tau \leq \\ &\leq 2M_R \alpha \Delta t, \end{aligned} \quad (46)$$

where the last inequality follows from (45). Choosing $\alpha > 0$ and $\Delta t > 0$ so that

$$\alpha \Delta t \leq \frac{\delta}{2M_R}, \quad (47)$$

and substituting (47) in (46) we obtain

$$\begin{aligned} |R(\mathbf{x}_i(t_k + \Delta t), \mathbf{x}_j(t_k + \Delta t)) - R(\mathbf{x}_i(t_k), \mathbf{x}_j(t_k))| &\leq \\ &\leq 2M_R \alpha \Delta t \leq 2M_R \frac{\delta}{2M_R} = \delta, \end{aligned} \quad (48)$$

completing the proof of (42).

Similarly, in order to associate the trust-region $\sigma > 0$ with the bound $\gamma > 0$ we first compute the time derivative of $\mathbf{r}_{\mathbf{x}(t),i}$ as follows

$$\dot{\mathbf{r}}_{\mathbf{x}(t),i} = \sum_{j \in \mathcal{D}_i \cup \{i\}} \frac{\partial \mathbf{r}_{\mathbf{x}(t),i}}{\partial \mathbf{x}_j} \dot{\mathbf{x}}_j. \quad (49)$$

Taking the absolute value of (49) and applying the triangle inequality yields

$$|\dot{\mathbf{r}}_{\mathbf{x}(t),i}| \leq \sum_{j \in \mathcal{D}_i \cup \{i\}} \left\| \frac{\partial \mathbf{r}_{\mathbf{x}(t),i}}{\partial \mathbf{x}_j} \right\| \|\dot{\mathbf{x}}_j\|. \quad (50)$$

Substituting (40) and (25) in (50) we obtain

$$|\dot{\mathbf{r}}_{\mathbf{x}(t),i}| \leq \sum_{j \in \{\mathcal{D}_i \cup i\}} M_r \alpha \leq NM_r \alpha, \quad (51)$$

where the last inequality is due to the fact that $|\{\mathcal{D}_i \cup i\}| \leq N$, where $|\cdot|$ stands for the cardinality of a

set. Expressing the difference $|\mathbf{r}_{\mathbf{x}_i(t_k+\Delta t),i} - \mathbf{r}_{\mathbf{x}_i(t_k),i}|$ as a definite integral, we have

$$\begin{aligned} |\mathbf{r}_{\mathbf{x}(t_k+\Delta t),i} - \mathbf{r}_{\mathbf{x}(t_k),i}| &= \left| \int_{t_k}^{t_k+\Delta t} \dot{\mathbf{r}}_{\mathbf{x}(\tau),i} d\tau \right| \leq \\ &\leq \int_{t_k}^{t_k+\Delta t} |\dot{\mathbf{r}}_{\mathbf{x}(\tau),i}| d\tau \leq NM_r \alpha \Delta t, \end{aligned} \quad (52)$$

where the last inequality holds due to (51).

Finally, selecting $\alpha > 0$ and $\Delta t > 0$ so that

$$\alpha \Delta t \leq \frac{\gamma}{NM_r}, \quad (53)$$

and substituting (53) in (52) we obtain

$$|\mathbf{r}_{\mathbf{x}(t_k+\Delta t),i} - \mathbf{r}_{\mathbf{x}(t_k),i}| \leq NM_r \frac{\gamma}{NM_r} \leq \gamma, \quad (54)$$

proving (43).

Combining (47) with (53) and using the fact that $\sigma \leq \alpha \Delta t$ (see also Section 4), we obtain (41), as desired. \square

Proposition 8, along with the following two results, can be used to characterize the performance of communications captured by the violations of the communication constraints (8) due to robot mobility. In particular, Proposition 9 shows that the dual iterates $\boldsymbol{\lambda}(t_k)$ converge to a neighborhood of the optimal Lagrange multipliers $\boldsymbol{\lambda}_{\mathbf{x}(t_k)}^*$ whose size can be reduced by decreasing the bounds δ and γ . A conceptually similar result is presented in Proposition 10 showing that the constraint violation can be made arbitrarily small through decreasing the problem parameters δ and γ . However, Proposition 8 implies that small values of the upper bounds δ and γ require a sufficiently small trust-region σ , robot speeds α , and time intervals Δt , with $\sigma \leq \alpha \Delta t$. Conversely, by decreasing the parameters in $\sigma \leq \alpha \Delta t$ we can select small enough values for δ and γ that ensure small constraint violations. Note that these results should be interpreted in an existential way, since values for the parameters of our problem are difficult to obtain. The proof of Proposition 9 is adapted from [22] and is presented in the Appendix for completeness. The proof of Proposition 10 can be found in [22] and is omitted.

Proposition 9 *Let $\mathbf{x}(t_k)$ denote the network configuration at time t_k , $\boldsymbol{\lambda}_{\mathbf{x}(t_k)}^*$ the associated optimal dual variables, and $\boldsymbol{\lambda}(t_k)$ the dual iterates obtained through the primal-dual iteration (17)-(18). Assume that the step size in (18) is bounded as $\epsilon \leq \frac{1}{M}$, and that differences between the channel reliabilities and the average rates of information generated at the sensors are absolutely bounded as defined in (8). Then, if assumptions (a)-(d) hold, the*

error between the dual iterate $\boldsymbol{\lambda}(t_k)$ and the optimal dual variable $\boldsymbol{\lambda}_{\mathbf{x}(t_k)}^$ is bounded by:*

$$\begin{aligned} \|\boldsymbol{\lambda}_{\mathbf{x}(t_k)}^* - \boldsymbol{\lambda}(t_k)\| &\leq \beta^k \|\boldsymbol{\lambda}(t_0) - \boldsymbol{\lambda}_{\mathbf{x}(t_0)}^*\| \\ &\quad + \sqrt{\frac{2\lambda_{\max}}{m(1-\beta)^2}} (N\delta + \gamma), \end{aligned} \quad (55)$$

where the constant β is defined as $\beta = \sqrt{\frac{1}{1+m\epsilon}}$.

Proposition 10 *Under the assumptions of Proposition 9, the norm of the constraint violation can be bounded as follows*

$$\begin{aligned} &\mathbb{P} [\mathbf{r}_{\mathbf{x}(t_k)} - \mathbf{A}_{\mathbf{x}(t_k)} \mathbf{t}(t_k)] \\ &\leq M\beta^k \|\boldsymbol{\lambda}(t_0) - \boldsymbol{\lambda}_{\mathbf{x}(t_0)}^*\| + \sqrt{\frac{2M^2\lambda_{\max}}{m(1-\beta)^2}} (N\delta + \gamma). \end{aligned} \quad (56)$$

6 Simulation Studies

In this section we provide a simulation study to illustrate our proposed method. All optimization problems are solved in Matlab using the CVX toolbox [40]. Specifically, we consider a coverage task that involves a mobile robot network consisting of $N = 14$ robots and $K = 2$ APs. The area of interest is a square with side equal to 2 units of length and the density function $\phi(\mathbf{q})$ is given by the following Gaussian mixture model

$$\phi(\mathbf{q}) = \sum_{i=1}^2 0.5N(\boldsymbol{\mu}_i, \boldsymbol{\Sigma}_i), \quad (57)$$

where $N(\boldsymbol{\mu}_i, \boldsymbol{\Sigma}_i)$ stands for a normal distribution with mean value $\boldsymbol{\mu}_i$ and covariance matrix $\boldsymbol{\Sigma}_i$. In particular, we select

$$\boldsymbol{\mu}_1 = [2, 2]^T, \quad \boldsymbol{\Sigma}_1 = \begin{bmatrix} 2 & 0 \\ 0 & 2 \end{bmatrix},$$

$$\boldsymbol{\mu}_2 = [0.1, 0.1]^T, \quad \boldsymbol{\Sigma}_2 = \begin{bmatrix} 2 & 0 \\ 0 & 9 \end{bmatrix}.$$

Given the density function (57), the ϕ -weighted area of \mathcal{A} is $\int_{\mathcal{A}} \phi(\mathbf{q}) d\mathbf{q} = 0.64$ area units.

The channel reliability $R(\mathbf{x}_i, \mathbf{x}_j)$ is modeled as a decreasing function of the distance between nodes i and j , i.e.,

$$R(\mathbf{x}_i, \mathbf{x}_j) = \begin{cases} 1 & \text{if } \|\mathbf{x}_{ij}\| < l \\ \sum_{p=0}^3 a_p \|\mathbf{x}_{ij}\|^p & \text{if } l < \|\mathbf{x}_{ij}\| \leq u, \\ 0 & \text{if } \|\mathbf{x}_{ij}\| > u \end{cases} \quad (58)$$

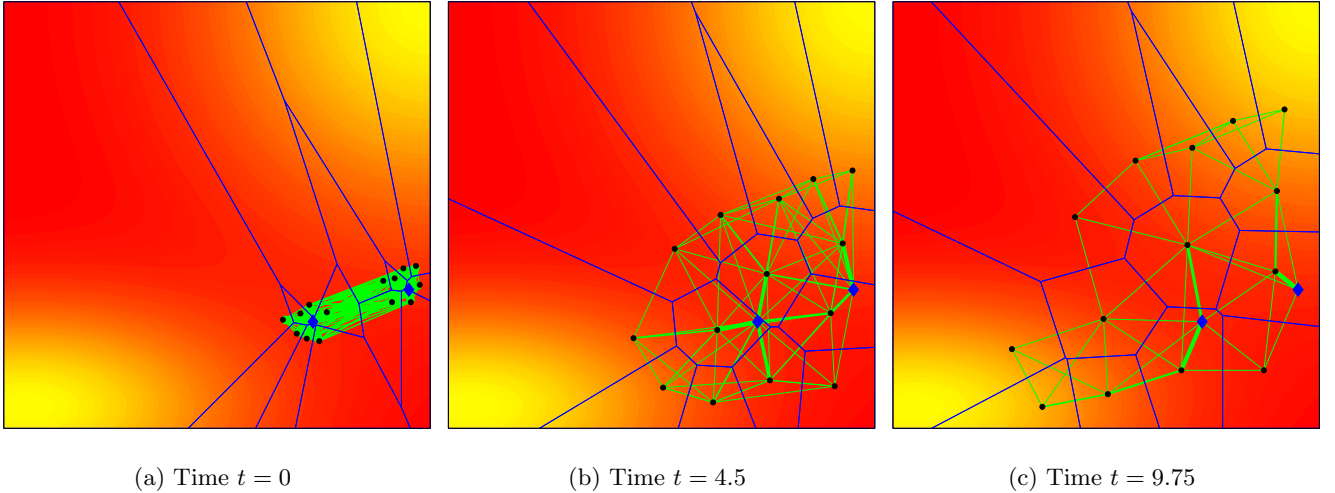


Fig. 2. Evolution of a communication network consisting of $N = 14$ robots (black dots) and $K = 2$ AP (blue rhombuses) during an area coverage task. Figures 2(a) through 2(c) show the evolution of the system at different time instants. Green lines represent the communication links among the nodes. Their thickness depends on the value of $T_{ij}R(\mathbf{x}_i, \mathbf{x}_j)$, i.e., thicker lines capture higher values. A presence of two sources in the upper right and bottom left corner of the area is captured by a higher density depicted in yellow.

where $\|x_{ij}\| = \|\mathbf{x}_i - \mathbf{x}_j\|$ and the constants a_p , $p = 0, \dots, 3$ are chosen so that $R(\mathbf{x}_i, \mathbf{x}_j)$ is a differentiable function. Notice that the model in (58) is a rough but reasonable approximation of the channel quality. In practice, an accurate estimation of the channel reliability is hard to obtain, as it depends on path loss that is a function of the distance between the source and the receiver, shadowing due to the existence of obstacles in the propagation path, and multi-path fading due to reflections, which are difficult to predetermine. A more sophisticated way to obtain the channel quality is presented in [41], where it is shown that $R(\mathbf{x}_i, \mathbf{x}_j)$ is indeed a decreasing function of the distance between nodes. In the following simulation studies, the limits l, u in (58) are selected to be equal to 0.3 and 0.6 units, respectively. In what follows, we examine the impact of the trust region σ and robot velocities α on the performance of the proposed distributed algorithm. In the rest of this section, we select the time interval Δt to be 10^{-2} time units.

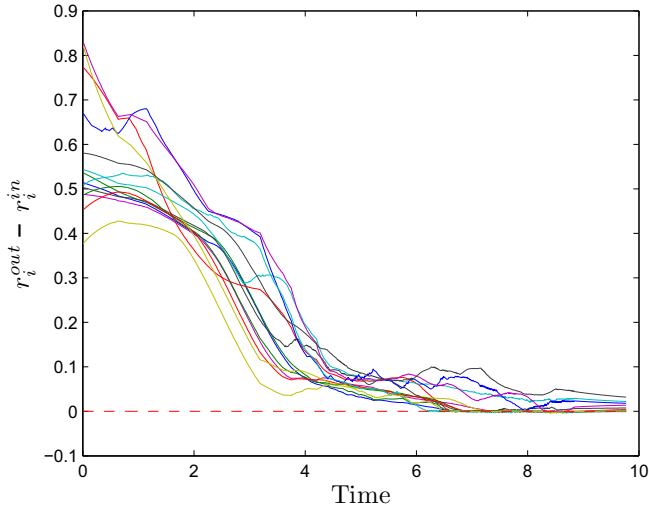
First, we select the robot velocity α to be equal to 10^{-1} and the trust region to be $\sigma = \alpha\Delta t = 10^{-3}$. Fig. 2 depicts the network at different instances of its evolution along with the quality of the communication links when α and σ are selected as mentioned above. As the diameter of the region of interest is approximately 4 times the value of u , multi-hop communication is necessary in order to cover the whole area as shown in Fig. 2. In Fig. 3(a), the quantity $r_i^{out} - r_i^{in}$ is plotted with respect to time showing that the robots are able to maintain integrity of the communication network, as defined by equation (8). Moreover, in Fig. 4 we show the average rate at which every robot generates information, where the higher rates correspond to robots that are close to the top right and bottom left corner in Fig. 2(c) due to

their proximity to the sources. In Fig. 6 the coverage objective function is depicted, showing that it increases monotonically as long as feasible routing variables exist and Fig. 5 shows the evolution of the Lagrange multipliers during network deployment.

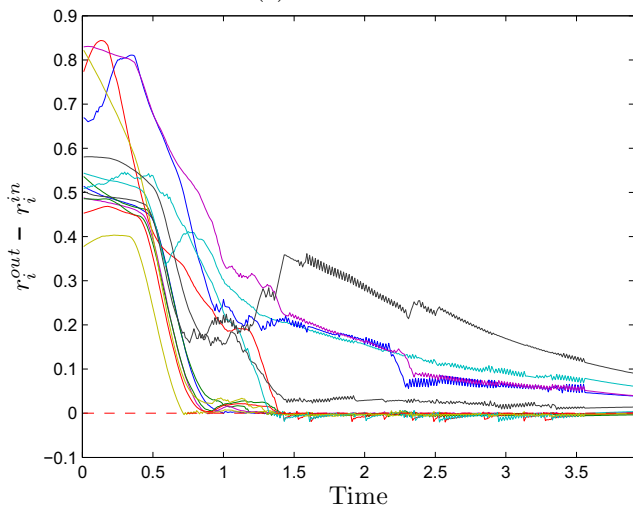
Second, we increase the robot velocity and the trust region, which are now selected as $\alpha = 5 \times 10^{-1}$ and $\sigma = \alpha\Delta t = 5 \times 10^{-3}$. The quantity $r_i^{out} - r_i^{in}$ and the coverage objective are plotted with respect to time in Figures 3(b) and 6, respectively. Notice in Figures 3(a) and 3(b) that as we increase the trust region and the robot velocity the constraint violation increases, which is in agreement with the results shown in Propositions 8 and 10. Specifically, as we increase α and σ , larger values for the parameters δ and γ must be selected due to (41), in Proposition 8, which implies a larger constraint violation due to Proposition 10. Also, due to this larger constraint violation, the robots stay motionless for a larger percentage of the time required for convergence, as shown in Figure 7, until feasible routing variables are obtained by the primal-dual algorithm (17)-(18). Observe also in Figure 6 that the total time required for convergence of the algorithm decreases as we increase the trust region and the robot velocity, since in doing so, the robots are allowed to move more during the time interval (t_k, t_{k+1}) . Moreover, in Figure 6, notice that the coverage performance when the network has converged to the final configuration is quite satisfactory, since it is very close to the ϕ -weighted area of \mathcal{A} .

7 Conclusions

In this paper, we presented a distributed control scheme for maximizing the area coverage by a mobile sensor net-



(a) $\sigma = 10^{-3}$



(b) $\sigma = 5 \times 10^{-3}$

Fig. 3. Graphical depiction of the difference $r_i^{out} - r_i^{in}$ for all robots of the network when the trust region size is $\sigma = 10^{-3}$ (Figure 3(a)) and $\sigma = 5 \times 10^{-3}$ (Figure 3(b)).

work and at the same time ensuring that packets of information are reliably relayed to a set of APs. The information generated by the sensors depends on both their sensing capabilities and the frequency at which events occur in their vicinity. This information is then routed to the APs through a multi-hop network whose communication links modeled channel reliabilities. A hybrid scheme was proposed that decouples the optimization of the coverage objective from the control of the communication variables. Particularly, the update of the communication variables was performed periodically in the dual domain and was followed by robot mobility due to a distributed sequential concave program designed to optimize the coverage objective. Simulation studies verified the efficacy of the proposed method.

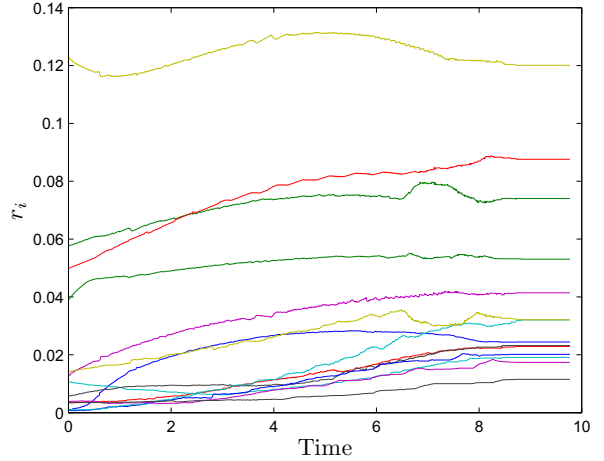


Fig. 4. Graphical representation of the average rate r_i for all robots of the network when $\sigma = 10^{-3}$.

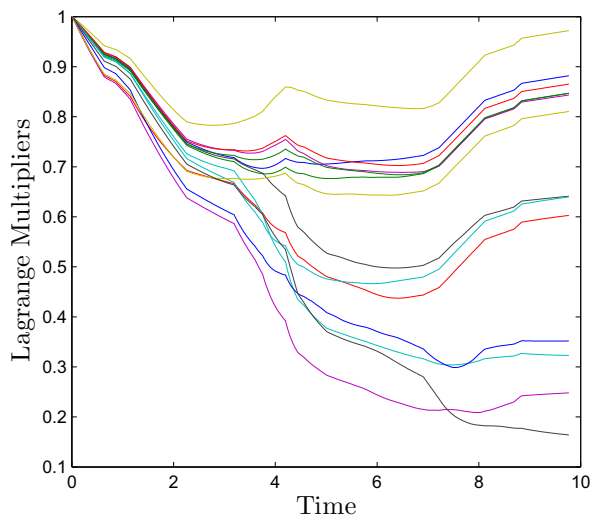


Fig. 5. Evolution of Lagrange multipliers for all robots when $\sigma = 10^{-3}$.

A Appendix

A.1 Proof of Proposition 9

The proof is similar to the proof of Theorem 1 in [22]. The difference with that proof lies in that here the rates of information $\mathbf{r}_{\mathbf{x}}$ generated at the sensors depend on the position of the robots \mathbf{x} and are not determined by the primal-dual algorithm (17)-(18). Following a similar analysis, we can apply the triangle inequality to bound the distance $\|\boldsymbol{\lambda}_{\mathbf{x}(t_{k+1})}^* - \boldsymbol{\lambda}(t_k)\|$ as

$$\|\boldsymbol{\lambda}(t_{k+1}) - \boldsymbol{\lambda}_{\mathbf{x}(t_{k+1})}^*\| \leq \|\boldsymbol{\lambda}(t_{k+1}) - \boldsymbol{\lambda}_{\mathbf{x}(t_k)}^*\| + \|\boldsymbol{\lambda}_{\mathbf{x}(t_{k+1})}^* - \boldsymbol{\lambda}_{\mathbf{x}(t_k)}^*\|. \quad (\text{A.1})$$

To simplify notation, denote the spatial configuration at time instants t_k and t_{k+1} by \mathbf{x} and \mathbf{y} , respectively. In what follows, we first derive a bound on the second term

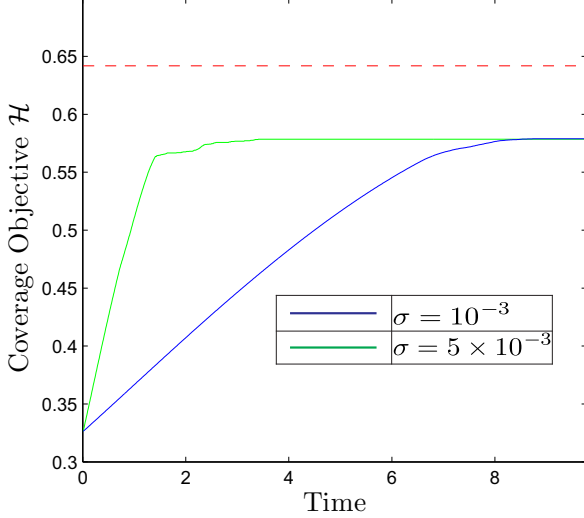


Fig. 6. Evolution of the coverage objective function \mathcal{H} when the trust region size is $\sigma = 10^{-3}$ (blue line) and $\sigma = 5 \times 10^{-3}$ (green line). The red dashed line stands for the ϕ -weighted area of \mathcal{A} .

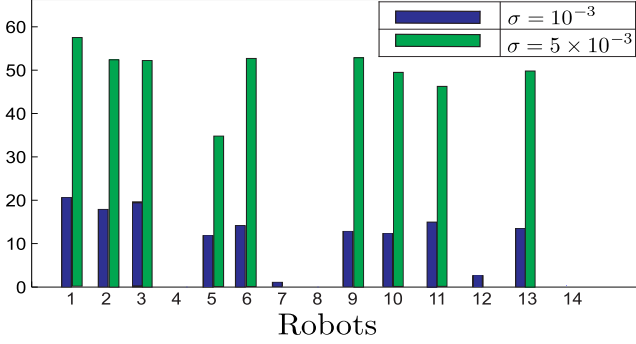


Fig. 7. Percentage of time required for convergence that each robot remains stationary due to violations of the communication constraint, for two different trust regions.

of (A.1). Since the dual function is strongly convex by assumption (A1), we have that

$$g_{\mathbf{x}}(\boldsymbol{\lambda}_{\mathbf{y}}^*) \geq g_{\mathbf{x}}(\boldsymbol{\lambda}_{\mathbf{x}}^*) + \nabla g_{\mathbf{x}}(\boldsymbol{\lambda}_{\mathbf{x}}^*)^T (\boldsymbol{\lambda}_{\mathbf{y}}^* - \boldsymbol{\lambda}_{\mathbf{x}}^*) + \frac{m}{2} \|\boldsymbol{\lambda}_{\mathbf{x}}^* - \boldsymbol{\lambda}_{\mathbf{y}}^*\|^2. \quad (\text{A.2})$$

Moreover, since $\boldsymbol{\lambda}_{\mathbf{x}}^*$ is the minimizer of the convex function $g_{\mathbf{x}}(\boldsymbol{\lambda})$, we have that $\nabla g_{\mathbf{x}}(\boldsymbol{\lambda}_{\mathbf{x}}^*)^T (\boldsymbol{\lambda}_{\mathbf{y}}^* - \boldsymbol{\lambda}_{\mathbf{x}}^*) \geq 0$ and, therefore, (A.2) yields

$$g_{\mathbf{x}}(\boldsymbol{\lambda}_{\mathbf{y}}^*) \geq g_{\mathbf{x}}(\boldsymbol{\lambda}_{\mathbf{x}}^*) + \frac{m}{2} \|\boldsymbol{\lambda}_{\mathbf{x}}^* - \boldsymbol{\lambda}_{\mathbf{y}}^*\|^2. \quad (\text{A.3})$$

Similarly, we obtain that

$$g_{\mathbf{y}}(\boldsymbol{\lambda}_{\mathbf{x}}^*) \geq g_{\mathbf{y}}(\boldsymbol{\lambda}_{\mathbf{y}}^*) + \frac{m}{2} \|\boldsymbol{\lambda}_{\mathbf{x}}^* - \boldsymbol{\lambda}_{\mathbf{y}}^*\|^2. \quad (\text{A.4})$$

Adding the inequalities (A.3) and (A.4) and solving for

$\|\boldsymbol{\lambda}_{\mathbf{x}}^* - \boldsymbol{\lambda}_{\mathbf{y}}^*\|^2$, we get

$$\|\boldsymbol{\lambda}_{\mathbf{x}}^* - \boldsymbol{\lambda}_{\mathbf{y}}^*\|^2 \leq \frac{1}{m} [g_{\mathbf{x}}(\boldsymbol{\lambda}_{\mathbf{y}}^*) - g_{\mathbf{y}}(\boldsymbol{\lambda}_{\mathbf{y}}^*) + g_{\mathbf{y}}(\boldsymbol{\lambda}_{\mathbf{x}}^*) - g_{\mathbf{x}}(\boldsymbol{\lambda}_{\mathbf{x}}^*)]. \quad (\text{A.5})$$

Note that $\boldsymbol{\lambda}_{\mathbf{x}}^*$ is the optimal Lagrange multiplier of the dual function $g_{\mathbf{x}}(\boldsymbol{\lambda})$ associated with the robots' position \mathbf{x} . Define by $\mathbf{t}_{\mathbf{y}}(\boldsymbol{\lambda}_{\mathbf{x}}^*)$ the primal Lagrangian maximizer of the dual function associated with robot positions \mathbf{y} and multipliers $\boldsymbol{\lambda}_{\mathbf{x}}^*$. Then, we have

$$g_{\mathbf{y}}(\boldsymbol{\lambda}_{\mathbf{x}}^*) = f_0(\mathbf{t}_{\mathbf{y}}(\boldsymbol{\lambda}_{\mathbf{x}}^*)) + \boldsymbol{\lambda}_{\mathbf{x}}^{*T} (\mathbf{A}_{\mathbf{y}} \mathbf{t}_{\mathbf{y}}(\boldsymbol{\lambda}_{\mathbf{x}}^*) - \mathbf{r}_{\mathbf{y}}). \quad (\text{A.6})$$

For the same multipliers $\boldsymbol{\lambda}_{\mathbf{x}}^*$, consider that value of the dual function $g_{\mathbf{x}}(\boldsymbol{\lambda}_{\mathbf{x}}^*)$ associated with positions \mathbf{x} . Then, we have that

$$g_{\mathbf{x}}(\boldsymbol{\lambda}_{\mathbf{x}}^*) = \max_{\mathbf{t}} \left\{ f_0(\mathbf{t}) + \boldsymbol{\lambda}_{\mathbf{x}}^{*T} (\mathbf{A}_{\mathbf{x}} \mathbf{t} - \mathbf{r}_{\mathbf{x}}) \right\} \geq f_0(\mathbf{t}_{\mathbf{y}}(\boldsymbol{\lambda}_{\mathbf{x}}^*)) + \boldsymbol{\lambda}_{\mathbf{x}}^{*T} (\mathbf{A}_{\mathbf{x}} \mathbf{t}_{\mathbf{y}}(\boldsymbol{\lambda}_{\mathbf{x}}^*) - \mathbf{r}_{\mathbf{x}}). \quad (\text{A.7})$$

because given the optimal multiplier $\boldsymbol{\lambda}_{\mathbf{x}}^*$ for a spacial configuration \mathbf{x} , the maximum in (36) is attained when $\mathbf{t} = \mathbf{t}_{\mathbf{x}}(\boldsymbol{\lambda}_{\mathbf{x}}^*)$. Subtracting (A.7) from (A.6) we get

$$g_{\mathbf{y}}(\boldsymbol{\lambda}_{\mathbf{x}}^*) - g_{\mathbf{x}}(\boldsymbol{\lambda}_{\mathbf{x}}^*) \leq \boldsymbol{\lambda}_{\mathbf{x}}^{*T} (\mathbf{A}_{\mathbf{y}} - \mathbf{A}_{\mathbf{x}}) \mathbf{t}_{\mathbf{y}}(\boldsymbol{\lambda}_{\mathbf{x}}^*) - \boldsymbol{\lambda}_{\mathbf{x}}^{*T} (\mathbf{r}_{\mathbf{y}} - \mathbf{r}_{\mathbf{x}}). \quad (\text{A.8})$$

Following the same procedure, we obtain the following upper bound for the term $g_{\mathbf{x}}(\boldsymbol{\lambda}_{\mathbf{x}}^*) - g_{\mathbf{y}}(\boldsymbol{\lambda}_{\mathbf{y}}^*)$

$$g_{\mathbf{x}}(\boldsymbol{\lambda}_{\mathbf{y}}^*) - g_{\mathbf{y}}(\boldsymbol{\lambda}_{\mathbf{y}}^*) \leq \boldsymbol{\lambda}_{\mathbf{y}}^{*T} (\mathbf{A}_{\mathbf{x}} - \mathbf{A}_{\mathbf{y}}) \mathbf{t}_{\mathbf{x}}(\boldsymbol{\lambda}_{\mathbf{y}}^*) - \boldsymbol{\lambda}_{\mathbf{y}}^{*T} (\mathbf{r}_{\mathbf{x}} - \mathbf{r}_{\mathbf{y}}). \quad (\text{A.9})$$

Substituting the inequalities (A.8) and (A.9) in (A.5) we get

$$\begin{aligned} \|\boldsymbol{\lambda}_{\mathbf{x}}^* - \boldsymbol{\lambda}_{\mathbf{y}}^*\|^2 &\leq \frac{1}{m} \left[\boldsymbol{\lambda}_{\mathbf{y}}^{*T} (\mathbf{A}_{\mathbf{x}} - \mathbf{A}_{\mathbf{y}}) \mathbf{t}_{\mathbf{x}}(\boldsymbol{\lambda}_{\mathbf{y}}^*) + \boldsymbol{\lambda}_{\mathbf{x}}^{*T} (\mathbf{A}_{\mathbf{y}} - \mathbf{A}_{\mathbf{x}}) \mathbf{t}_{\mathbf{y}}(\boldsymbol{\lambda}_{\mathbf{x}}^*) \right] \\ &\quad - \frac{1}{m} \left[\boldsymbol{\lambda}_{\mathbf{y}}^{*T} (\mathbf{r}_{\mathbf{x}} - \mathbf{r}_{\mathbf{y}}) + \boldsymbol{\lambda}_{\mathbf{x}}^{*T} (\mathbf{r}_{\mathbf{y}} - \mathbf{r}_{\mathbf{x}}) \right] \\ &\leq \frac{1}{m} \left[\left| \boldsymbol{\lambda}_{\mathbf{y}}^{*T} (\mathbf{A}_{\mathbf{x}} - \mathbf{A}_{\mathbf{y}}) \mathbf{t}_{\mathbf{x}}(\boldsymbol{\lambda}_{\mathbf{y}}^*) \right| + \left| \boldsymbol{\lambda}_{\mathbf{x}}^{*T} (\mathbf{A}_{\mathbf{y}} - \mathbf{A}_{\mathbf{x}}) \mathbf{t}_{\mathbf{y}}(\boldsymbol{\lambda}_{\mathbf{x}}^*) \right| \right] \\ &\quad + \frac{1}{m} \left[\left| \boldsymbol{\lambda}_{\mathbf{y}}^{*T} (\mathbf{r}_{\mathbf{x}} - \mathbf{r}_{\mathbf{y}}) \right| + \left| \boldsymbol{\lambda}_{\mathbf{x}}^{*T} (\mathbf{r}_{\mathbf{y}} - \mathbf{r}_{\mathbf{x}}) \right| \right] \quad (\text{A.10}) \end{aligned}$$

For the first term in the last inequality in (A.10), it holds that (cf. Lemma 1 in [22])

$$\left| \boldsymbol{\lambda}_{\mathbf{y}}^{*T} (\mathbf{A}_{\mathbf{x}} - \mathbf{A}_{\mathbf{y}}) \mathbf{t}_{\mathbf{x}}(\boldsymbol{\lambda}_{\mathbf{y}}^*) \right| + \left| \boldsymbol{\lambda}_{\mathbf{x}}^{*T} (\mathbf{A}_{\mathbf{y}} - \mathbf{A}_{\mathbf{x}}) \mathbf{t}_{\mathbf{y}}(\boldsymbol{\lambda}_{\mathbf{x}}^*) \right| \leq 2N \lambda_{\max} \delta. \quad (\text{A.11})$$

To bound the second term in that inequality in (A.10) we utilize equation (43). Specifically, equation (43) can be written in vector form as

$$|\mathbf{r}_x - \mathbf{r}_y| \leq \gamma \mathbf{1}, \quad (\text{A.12})$$

where $\mathbf{1}$ is vector with all entries equal to 1 and the absolute value is taken element-wise on vector $\mathbf{r}_x - \mathbf{r}_y$. Therefore, for any $\boldsymbol{\lambda}$ we have that

$$\left| \boldsymbol{\lambda}^T (\mathbf{r}_x - \mathbf{r}_y) \right| \leq \gamma \boldsymbol{\lambda}^T \mathbf{1} \leq \gamma \lambda_{\max}, \quad (\text{A.13})$$

where in the second inequality we have used the fact that because all components of $\boldsymbol{\lambda}$ are non-negative, $\boldsymbol{\lambda}^T \mathbf{1} = \|\boldsymbol{\lambda}\|_1 \leq \lambda_{\max}$.

Substituting (A.11) and (A.13) into (A.10) yields

$$\|\boldsymbol{\lambda}_x^* - \boldsymbol{\lambda}_y^*\|^2 \leq \frac{2\lambda_{\max}}{m} (N\delta + \gamma). \quad (\text{A.14})$$

Next, in order to bound the first term of (A.1), the result of (Lemma 2, [22]) is utilized. According to this Lemma it holds that:

$$\left\| \boldsymbol{\lambda}(t_{k+1}) - \boldsymbol{\lambda}_{\mathbf{x}(t_k)}^* \right\|^2 \leq \beta^2 \left\| \boldsymbol{\lambda}(t_k) - \boldsymbol{\lambda}_{\mathbf{x}(t_k)}^* \right\|^2 \quad (\text{A.15})$$

Plugging equations (A.14) and (A.15) into (A.1) yields the following:

$$\begin{aligned} \left\| \boldsymbol{\lambda}_{\mathbf{x}(t_k)}^* - \boldsymbol{\lambda}(t_k) \right\| &\leq \beta \left\| \boldsymbol{\lambda}(t_k) - \boldsymbol{\lambda}_{\mathbf{x}(t_k)}^* \right\| \\ &+ \sqrt{\frac{2\lambda_{\max}}{m} (N\delta + \gamma)}. \end{aligned} \quad (\text{A.16})$$

Applying the above inequality recursively between the $k+1$ iteration and 0 yields:

$$\begin{aligned} \left\| \boldsymbol{\lambda}_{\mathbf{x}(t_k)}^* - \boldsymbol{\lambda}(t_k) \right\| &\leq \beta^{k+1} \left\| \boldsymbol{\lambda}(t_k) - \boldsymbol{\lambda}_{\mathbf{x}(t_k)}^* \right\| \\ &+ \sum_{e=0}^k \beta^e \sqrt{\frac{2\lambda_{\max}}{m} (N\delta + \gamma)}. \end{aligned} \quad (\text{A.17})$$

Observing that $\sum_{e=0}^k \beta^e \leq \sum_{e=0}^{\infty} \beta^e = \frac{1}{1-\beta}$ and shifting the time from t_{k+1} to t_k yields the result in (55), completing the proof.

References

[1] Y. Kantaros and M. M. Zavlanos, "Distributed simultaneous coverage and communication control by mobile sensor

networks," in *2nd IEEE Global Conference on Signal and Information Processing (GlobalSIP)*, Atlanta, GA, USA, December 2014, pp. 833–837.

- [2] —, "Communication-aware coverage control for robotic sensor networks," in *53rd IEEE Conference on Decision and Control*, Los Angeles, CA, USA, December 2014, pp. 6863–6865.
- [3] J. Cortés, S. Martínez, T. Karatas, and F. Bullo, "Coverage control for mobile sensing networks," *IEEE Transactions on Robotics and Automation*, vol. 20, no. 2, pp. 243–255, 2004.
- [4] J. Cortés, S. Martínez, and F. Bullo, "Spatially-distributed coverage optimization and control with limited-range interactions," *ESAIM: Control, Optimisation and Calculus of Variations*, vol. 11, no. 4, pp. 691–719, 2005.
- [5] M. Zhu and S. Martínez, "Distributed coverage games for energy-aware mobile sensor networks," *SIAM Journal on Control and Optimization*, vol. 51, no. 1, pp. 1–27, 2013.
- [6] A. Gusrialdi, T. Hatanaka, and M. Fujita, "Coverage control for mobile networks with limited-range anisotropic sensors," in *47th IEEE Conference on Decision and Control*, Cancun, Mexico, December 2008, pp. 4263–4268.
- [7] B. Hessel, N. Chakraborty, and K. Sycara, "Coverage control for mobile anisotropic sensor networks," in *IEEE International Conference on Robotics and Automation*, Shanghai, May 2011, pp. 2878–2885.
- [8] Y. Stergiopoulos and A. Tzes, "Spatially distributed area coverage optimisation in mobile robotic networks with arbitrary convex anisotropic patterns," *Automatica*, vol. 49, no. 1, pp. 232–237, 2013.
- [9] —, "Cooperative positioning/orientation control of mobile heterogeneous anisotropic sensor networks for area coverage," in *IEEE International Conference on Robotics and Automation (ICRA)*, Hong Kong, China, June, 2014, pp. 1106–1111.
- [10] L. Pimenta, V. Kumar, R. C. Mesquita, and G. Pereira, "Sensing and coverage for a network of heterogeneous robots," in *47th IEEE Conference on Decision and Control*, Cancun, Mexico, December 2008, pp. 3947–3952.
- [11] C. Caicedo-Nuez and M. Zefran, "A coverage algorithm for a class of non-convex regions," in *47th IEEE Conference on Decision and Control*, Cancun, Mexico, December 2008, pp. 4244–4249.
- [12] A. Renzaglia, L. Doitsidis, A. Martinelli, and E. B. Kosmatopoulos, "Multi-robot three-dimensional coverage of unknown areas," *The International Journal of Robotics Research*, vol. 31, no. 6, pp. 738–752, 2012.
- [13] Y. Kantaros, M. Thanou, and A. Tzes, "Distributed coverage control for concave areas by a heterogeneous robot-swarm with visibility sensing constraints," *Automatica*, vol. 53, pp. 195–207, 2015.
- [14] Y. Kim and M. Mesbahi, "On maximizing the second smallest eigenvalue of a state-dependent graph laplacian," *IEEE Transactions on Automatic Control*, vol. 51, no. 1, pp. 116–120, 2006.
- [15] M. C. DeGennaro and A. Jadbabaie, "Decentralized control of connectivity for multi-agent systems," in *45th IEEE Conference on Decision and Control*, San Diego, CA, USA, December 2006, pp. 3628–3633.
- [16] M. M. Zavlanos and G. J. Pappas, "Potential fields for maintaining connectivity of mobile networks," *IEEE Transactions on Robotics*, vol. 23, no. 4, pp. 812–816, 2007.
- [17] S. Gil, D. Feldman, and D. Rus, "Communication coverage for independently moving robots," in *Intelligent Robots and*

- Systems (IROS), 2012 IEEE/RSJ International Conference on.* IEEE, 2012, pp. 4865–4872.
- [18] M. Zavlanos and G. Pappas, “Distributed connectivity control of mobile networks,” *IEEE Transactions on Robotics*, vol. 24, no. 6, pp. 1416–1428, 2008.
- [19] G. Notarstefano, K. Savla, F. Bullo, and A. Jadbabaie, “Maintaining limited-range connectivity among second-order agents,” in *American Control Conference*, Minneapolis, MN, USA, June 2006, pp. 6–pp.
- [20] M. Ji and M. B. Egerstedt, “Distributed coordination control of multi-agent systems while preserving connectedness.” *IEEE Transactions on Robotics*, vol. 23, no. 4, pp. 693–703, August 2007.
- [21] M. Zavlanos, M. Egerstedt, and G. Pappas, “Graph theoretic connectivity control of mobile robot networks,” *Proc. of the IEEE*, vol. 99, no. 9, pp. 1525–1540, 2011.
- [22] M. M. Zavlanos, A. Ribeiro, and G. J. Pappas, “Network integrity in mobile robotic networks,” *IEEE Transactions on Automatic Control*, vol. 58, no. 1, pp. 3–18, 2013.
- [23] —, “Mobility & routing control in networks of robots,” in *49th IEEE Conference on Decision and Control*, Atlanta, GA, USA, December 2010, pp. 7545–7550.
- [24] A. Ghaffarkhah and Y. Mostofi, “Communication-aware motion planning in mobile networks,” *IEEE Transactions on Automatic Control*, vol. 56, no. 10, pp. 2478–2485, 2011.
- [25] J. Le Ny, A. Ribeiro, and G. J. Pappas, “Adaptive communication-constrained deployment of unmanned vehicle systems,” *IEEE Journal on Selected Areas in Communications*, vol. 30, no. 5, pp. 923–934, 2012.
- [26] S. Gil, M. Schwager, B. J. Julian, and D. Rus, “Optimizing communication in air-ground robot networks using decentralized control,” in *Robotics and Automation (ICRA), 2010 IEEE International Conference on.* IEEE, 2010, pp. 1964–1971.
- [27] W. Jiang and M. Zefran, “Coverage control with information aggregation,” in *52nd IEEE Conference on Decision and Control*, Firenze, Italy, December 2013, pp. 5421–5426.
- [28] W. Li and C. G. Cassandras, “Distributed cooperative coverage control of sensor networks,” in *44th IEEE Conference on Decision and Control and European Control Conference*, Seville, Spain, December 2005, pp. 2542–2547.
- [29] Y. Stergiopoulos, Y. Kantaros, and A. Tzes, “Connectivity-aware coordination of robotic networks for area coverage optimization,” in *International Conference on Industrial Technology (ICIT)*. Athens, Greece: IEEE, March, 2012, pp. 31–35.
- [30] —, “Distributed Control of Mobile Sensor Networks under RF Connectivity Constraints,” *International Journal of Distributed Sensor Networks*, vol. 2012, 2012.
- [31] M. Bramson, *Stability of queueing networks*. Springer, 2008.
- [32] F. Bullo, J. Cortés, and S. Martinez, *Distributed Control of Robotic Networks*. Princeton University Press, 2009.
- [33] F. Aurenhammer and R. Klein, *Handbook of Computational Geometry*. Elsevier Publishing House, 1999, ch. 5: *Voronoi Diagrams*, pp. 201–290.
- [34] A. Ruszczyński, *Nonlinear optimization*. Princeton University Press, 2011, vol. 13.
- [35] D. P. Bertsekas and J. N. Tsitsiklis, *Parallel and distributed computation: numerical methods*. Prentice hall Englewood Cliffs, NJ, 1989, vol. 23.
- [36] N. Chatzipanagiotis, D. Dentcheva, and M. M. Zavlanos, “An augmented lagrangian method for distributed optimization,” *Mathematical Programming, Ser. A*, pp. 1–30, September 2014, (published online; DOI: 10.1007/s10107-014-0808-7).
- [37] J. Nocedal and S. J. Wright, *Numerical Optimization 2nd*. Springer, 2006.
- [38] S. Boyd and L. Vandenberghe, *Convex Optimization*. Cambridge University Press, 2004.
- [39] H. Flanders, “Differentiation under the integral sign,” *American Mathematical Monthly*, vol. 80, no. 6, pp. 615–627, 1973.
- [40] M. Grant and S. Boyd, “CVX: Matlab software for disciplined convex programming, version 2.1,” <http://cvxr.com/cvx>, Mar. 2014.
- [41] J. Fink, A. Ribeiro, and V. Kumar, “Robust control of mobility and communications in autonomous robot teams,” *Access, IEEE*, vol. 1, pp. 290–309, 2013.